Effect of Laser Energy and Vacuum Pressure on the Laser induce Plasma from Titanium Target

Muntazar shihab Ahmed
Laser science and technology, Department of Applied Sciences, University of Technology, Baghdad, Iraq.

Haider Abdulrida
Laser science and technology, Department of Applied Sciences, University of Technology, Baghdad, Iraq.

Qusay Adnan Abbas
Laser science and technology, Department of Applied Sciences, University of Technology, Baghdad, Iraq.

Email: as.20.72@grad.uotechnology.edu.iq ,100329@uotechnology.edu.iq, Qusay.a@Sc.Uobaghdad.edu.iq

Abstract

In this study, the effect of laser energy and vacuum pressure in Argon of laser induced spectroscopy from titanium target on the plasma emission and plasma parameter. The plasma was induced by Q-switched nanosecond Nd: YAG laser at three different energies (200, 300, 400 mJ). The laser induced plasma was applied in a vacuum chamber at different Ar pressures of 0.08, 0.2, and 0.4 Torr. The atomic and ionic emission lines increased in intensity directly with the laser energy. The plasma temperature determined according to Boltzmann-Plot, and the electron density (n_e) determined according to Saha-Boltzmann equation were increased with the laser energy. From the other hand, the T_e decreased with increasing the pressure as a result of increasing electron-atom collisions. The n_e increased with increasing the pressure from 0.08 to 0.2 and reduced at 0.4 Torr. The plasma parameters in Ar at different vacuum pressures from the Ti target at different laser energies were satisfied the plasma criteria.

Keywords: Plasma emission, LIPS, OES , Nano target, plasma characteristics, Debey-length, Debey number.

1. Introduction

Optical Emission Spectroscopy (OES) is a popular analytical technique that has wide-ranging applications such as determination of optimal growth parameters using glow discharge in deposition process [1], for the diagnostics of atmospheric plasmas relevant to bio-medical and environmental applications [2], and for atomic absorption and mass spectrometry [3]. It is also used as analytical method for steel, alloy, metal, geological studies. Laser induced plasma is one of the most widely used techniques for generating plasma from solid surfaces for optical emission spectrum analysis. This technique can be used to monitor the deposition process from contaminants or to diagnose the plasma to see its effect on the deposition process [4]. During the ablation process to create nanoparticles, the characteristics of the prepared nanoparticles can be controlled by varying the plasma parameters [5]. In addition to laser parameters such as laser flounce, wavelength, and pulse duration, the plasma processes for laser-induced plasma are extremely reliant on the surrounding media, and pressure during laser mater interaction [6].

Ciganovic et al, [7] studied the interaction of CO_2 laser at 10.6 μm and 100 ns pulses with a titanium implant in 0.1 mbar vacuum at different laser energies. The electron temperature was determined using the line -ratio method of 7535 K. The temperature was decreased by each subsequent laser pulse for the first few pulses. After ten laser pulses the temperature was steadied at 6000 K. Beside this the emission intensity indicate on reducing the ablation rate.

Liu et al, (2016) [8] studied laser induced plasma parameter and spectral intensities from Ti using Femtosecond plasma (100 fs, 800 nm) as a function of pressure (10 Pa to 10^4 Pa). The Ti atomic lines decay while the ionic ones grow with an increasing pressure. The increasing pressure slows the plasma expansion. The higher pressure will retard the plasma expansion, leading to larger electron density.

In this work, we study the effect of vacuum pressure and laser energy on the plasma characterization induced by Q-switched nano laser from titanium target.

2. Experimental

Titanium micro particles powder of 99.9% purity from Sigma-Aldrich Co. was pressed into a pellet of 1 cm diameter using a hydraulic piston under 5 tons press. Laser-induced plasma spectroscopy (LIPS) using a Q-switched Nd: YAG laser of 1064 nm wavelength, 10 ns pulse width, and 2 mm spot diameter at different energies of 200, 300, and 400 mJ, and Thorlabs compact spectrometer, (Type CCS 100/M) of $\Delta\lambda<0.5nm$ resolution at 320– 740 nm range, connected to PC-computer. A quartz lens was used to focus the laser beam at its focal length of 10 cm onto the target. The plasma emissions were collected by an optical fiber to be transmitted to the spectrometer fixed at a 5cm distance at a 45 ° angle with the target surface. The testing was done under three different vacuum stages in Ar of 8×10-2, 0.2, and 0.4 Torr. The chamber was vacuumed using a double-stage rotary pump (CIT-ALCATEL). A needle valve for gas admittance and a Perini gauge (Edward) was used to control the vacuum pressure of the chamber. Figure 1 shows a photograph of the used chamber. The crystalline structure of the target was examined using the XRD (Shimadzu XRD 6000) of wavelength λ= 1.5405 Å for Cu (Kα) emission.

Figure 1 : Photograph for Chamber used in experiment.

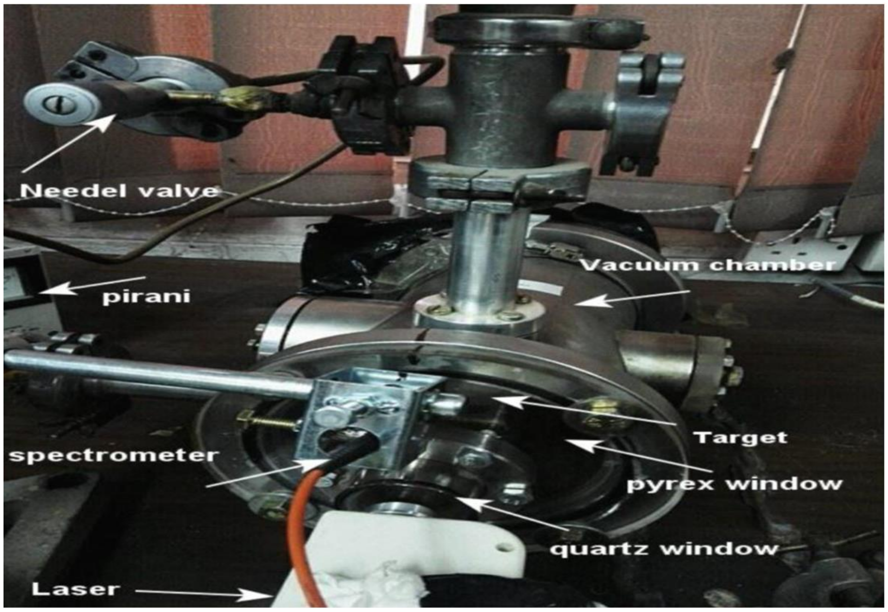

3. Results and discussions

Figure 3 illustrates the XRD curve for the pressed titanium target. A polycrystalline structure appeared with diffraction lines identical to diffraction from the planes (100), (002), (101), (102), (110), (103), (200), (112), and (201) of pure hexagonal phase for titanium corresponding to JCPDF No. 96-900-8518.

Figure 2: XRD pattern for the Ti target, the inset figure shows the used target.

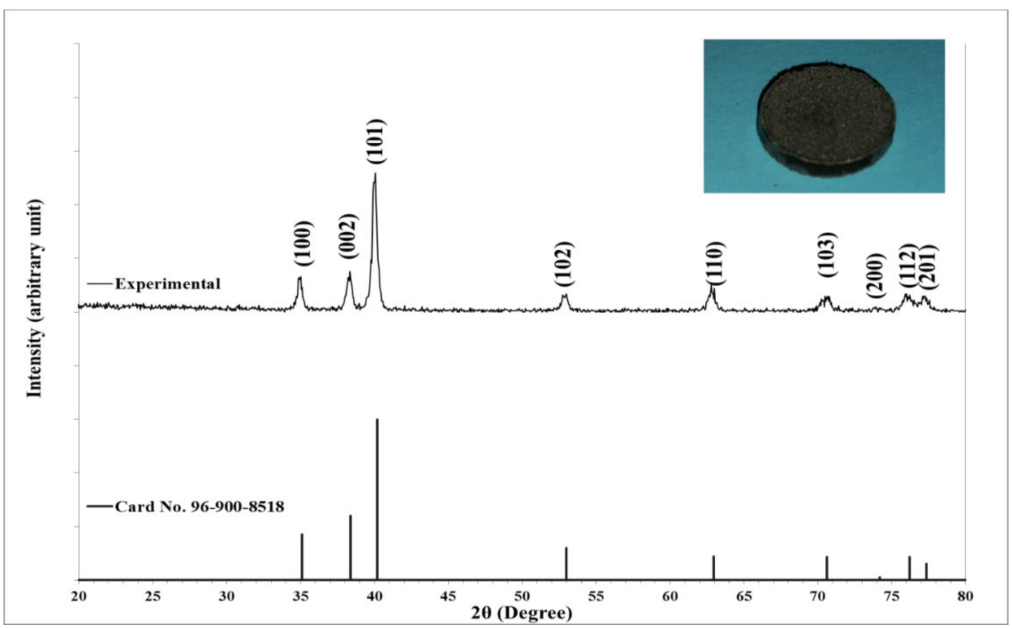

Figures 3 to 5 illustrate the spectroscopic patterns of plasma emitted induced by nano pulsed- laser in argon under different vacuum pressures 0.08, 0.2, and 0.4 Torr, respectively. The plasma is induced by different laser energies (200, 300, and 400 mJ) from Ti targets. The emitted lines have a good matching with the atomic and ionic standard lines of titanium (Ti-I and Ti-II) according to the NIST standard data [9]. The emission lines of the different wavelengths, in each pattern, differ in intensities due to their diverse transitions probability and statistical weight of the upper energy levels for each transition. The emitted lines for electronic transition in the atomic state are more intense than the ionic lines, indicating a partially ionized plasma.

The emission lines increased in intensity directly with the laser energy due to an increase in the ablated substances into the plasma column as a result of increasing the sputtering yield per pulse, these species with high-density act as emitted sources during the de-excitation of their excited atoms by the laser [10]. According to Stark's principle, the lines become more breadth with increasing laser energy, which suggests an increase in plasma density [11].

Figure 3: Emitted spectra from Ti target under 0.08 Torr vacuum induced by different laser energies

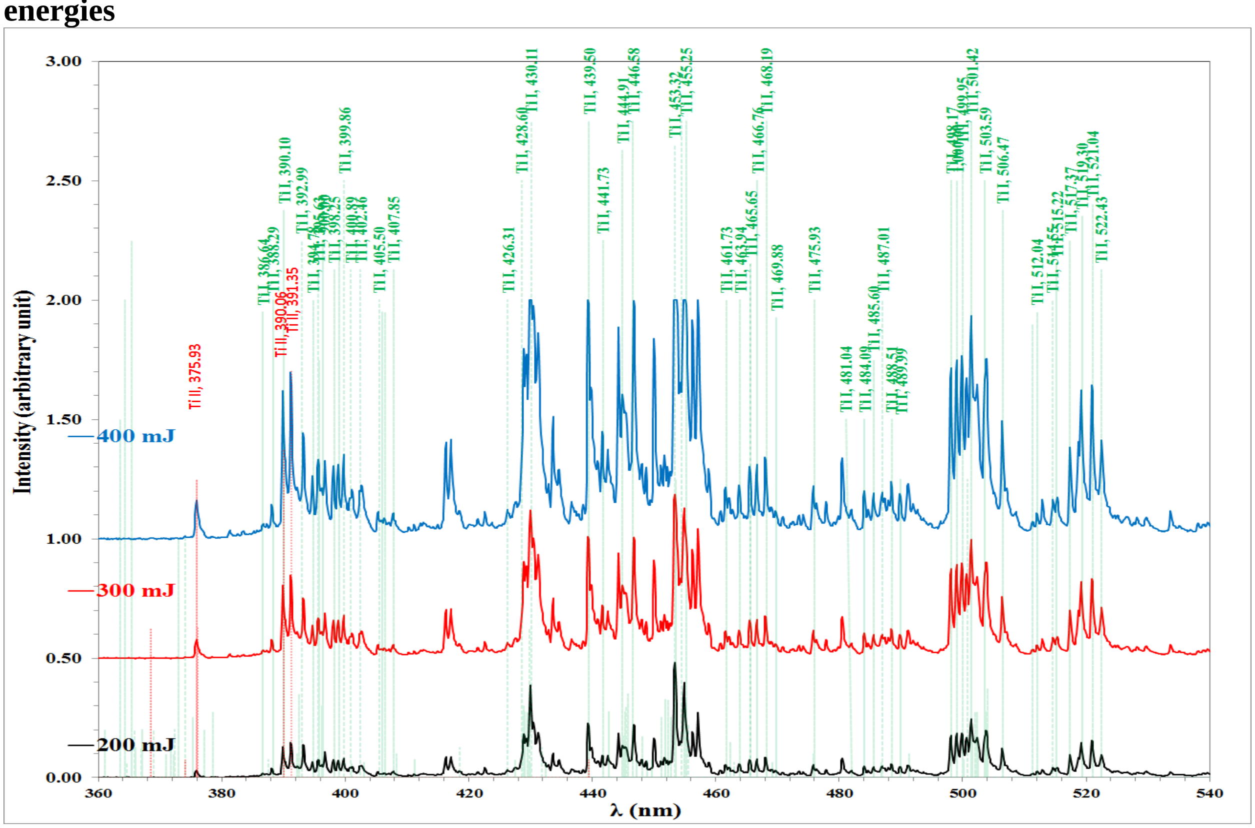

Figure 4: Emitted spectra from Ti target under 0.2 Torr vacuum induced by different laser energies

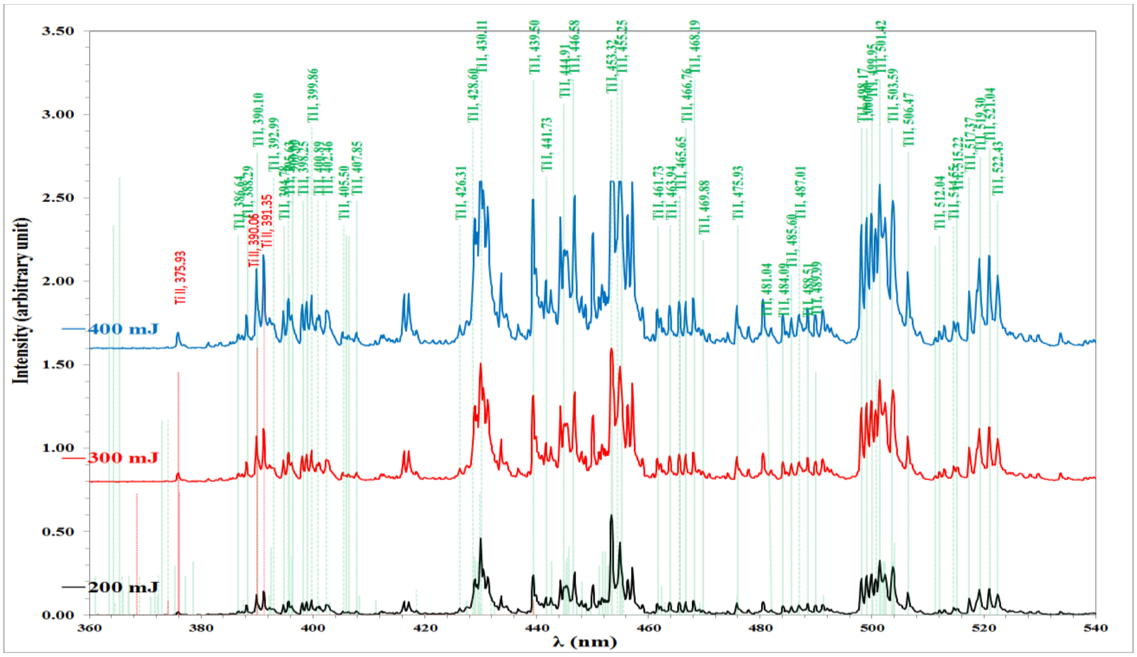

Figure 5: Emitted spectra from Ti target under 0.4 Torr vacuum induced by different laser energies

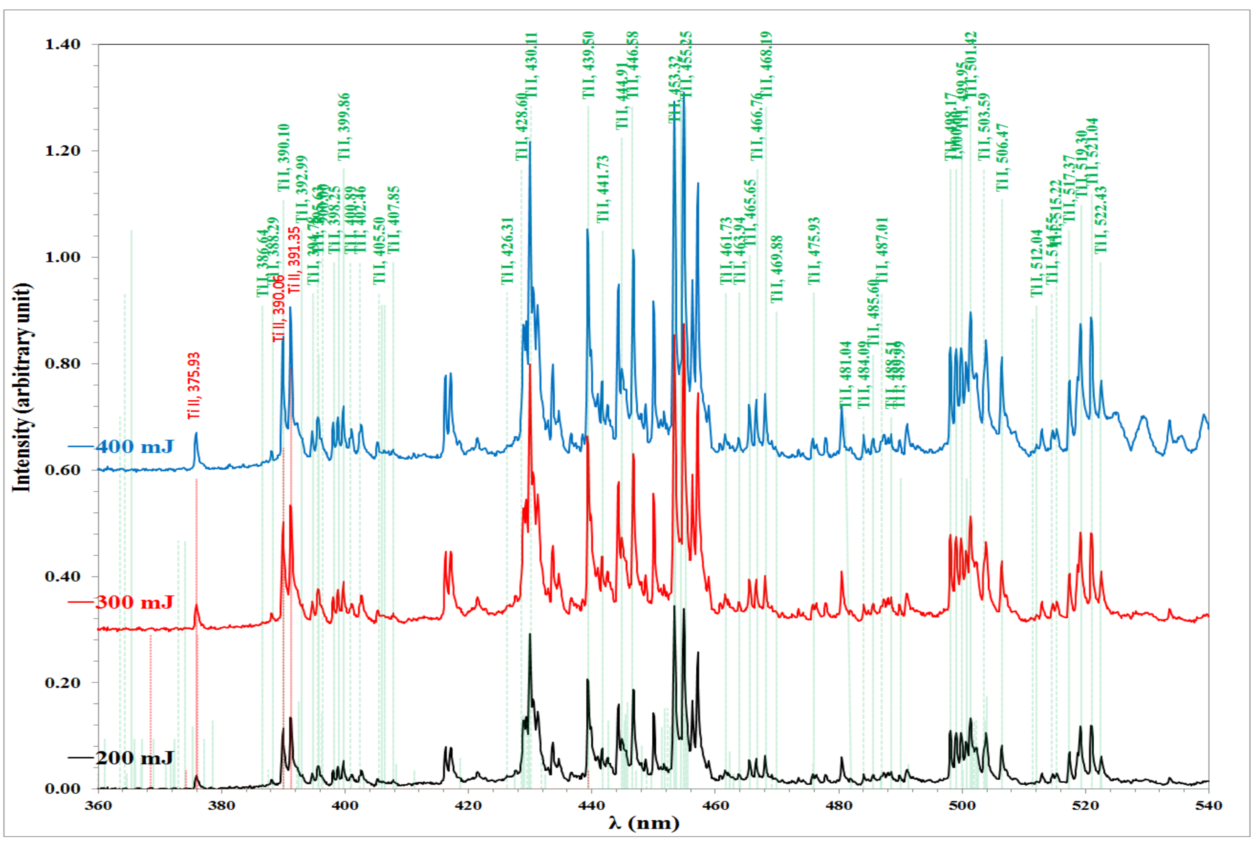

The mean values of electron temperature (T_e) at the different cases was determined using Boltzmann-Plot as shown in Figure 6, while the electron density (n_e) was determined according to Saha-Boltzmann equation [12].

$$n_e[cm^{-3}] = \frac{I_z^*}{I_{z+1}^*}\, 6.04 \times 10^{21} (T)^{3/2} \times exp[(-E_{k,z+1} + E_{k,z} - \chi_z)/k_\beta T]$$

where $I_z^* = I_Z\ \lambda_{ki,Z}/g_{k,Z}A_{ki,Z}$ and χ_z is the ionization energy of the species in the ionization stage z.

Figure 6: Boltzmann-plot for Ti I lines at different pulsed energies, under 0.08 (A), 0.2 (B) , and 0.4 Torr vacuum

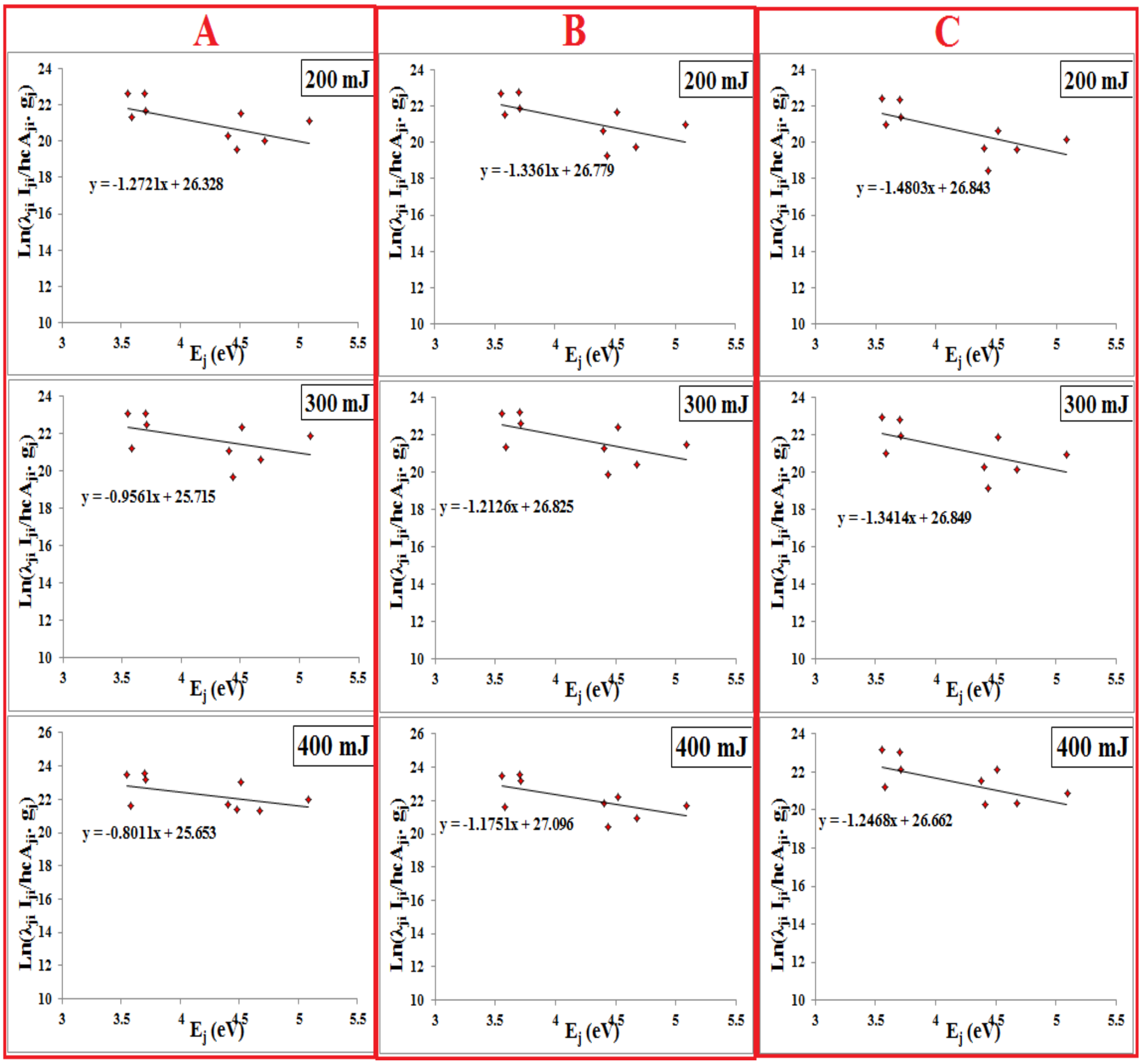

The variation of electron temperature (T_e) and electron density (n_e) with the laser energy under the three different vacuum levels were shown in Figure 7.

Figure 8: electron density and plasma temperature against laser energies, under 0.08 (A), 0.2 (B) , and 0.4 Torr vacuum.

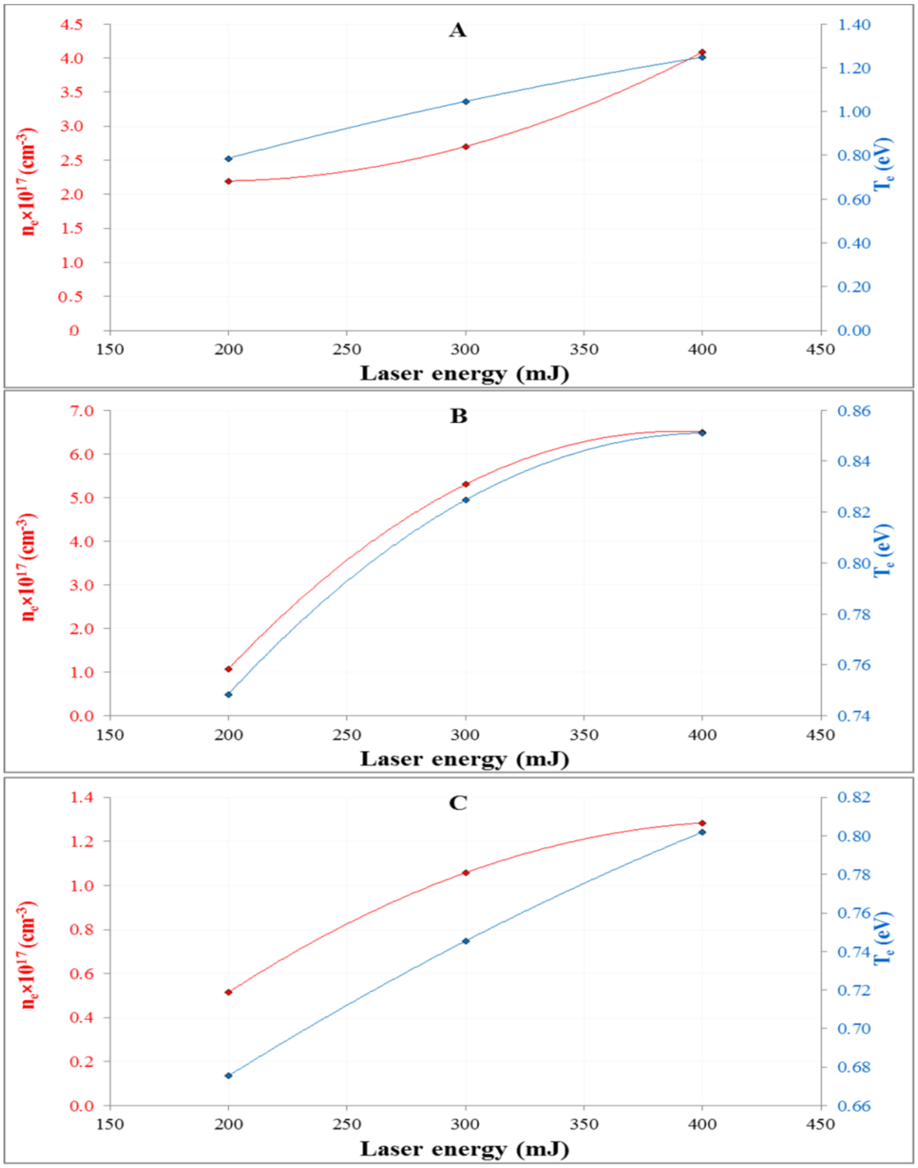

Table 1 listed the plasma parameters for laser-induced plasma in an argon environment at different vacuum pressure from the Ti target at different laser energies. All plasma parameters satisfy the plasma criteria, with high plasma frequency, short Debey-length, and large Debey number. Both T_e and ne increased with increasing the laser energy. On the other hand, the Te decreased with increasing pressure as a result of increasing electron-atom collisions. The n_e increased with increasing the pressure from 0.08 to 0.2 and reduced for more pressure at 0.4 Torr. Increasing the pressure to a certain extent leads to an increase in ionizing collisions between electrons with atoms. But at a pressure higher than that, it leads to an increase in non-ionizing collisions, which does not give enough time for the electrons to obtain sufficient energy to ionize the atom, thus reducing in collision cross-section, due to reducing the mean energy for plasma electrons [13].

Table 1: parameters of plasma induced from nano-Ti targets in Ar at different vacuum pressure, and different laser energies

P (Torr)	E (mJ)	T_e (eV)	$n_e \times 10^{17}$ (cm^{-3})	f_p (Hz) $\times 10^{12}$	λ_D *10^{-5}(cm)	N_d
0.08	**200**	0.786	2.19	13.301	0.445	809
	300	1.046	2.70	14.757	0.462	1118
	400	1.248	4.09	18.160	0.411	1185
0.2	**200**	0.745	1.07	2.937	1.965	3401
	300	0.825	5.30	6.537	0.927	1768
	400	0.851	6.50	7.240	0.850	1673
0.4	**200**	0.676	0.51	2.037	2.693	4206
	300	0.745	1.06	2.921	1.972	3400
	400	0.802	1.28	3.219	1.856	3443

The change of emission intensity for LIPS with laser energy at different vacuum pressures for the 453.32 nm wavelength Ti-I line is illustrated in Figure 9. The figure shows that the intensity of the emission spectrum increases with increasing laser energy. By comparing the intensity of laser-induced plasma emission at different vacuum pressures, we notice that the intensity increases when the pressure is increased from 0.08 to 0.2 Torr and decreases with more increasing at 0.4 Torr, with the same behavior for all laser energies. The results indicate that the optimum pressure for the LIPS process is at 0.2 Torr vacuum pressure from the Ti target in Ar, with the highest laser breakdown process.

Figure 9: variation of emission intensity of Ti I (453.32 nm) with laser energies under different vacuum (2, 4, and 0.4 Torr) in Ar from the three different targets.

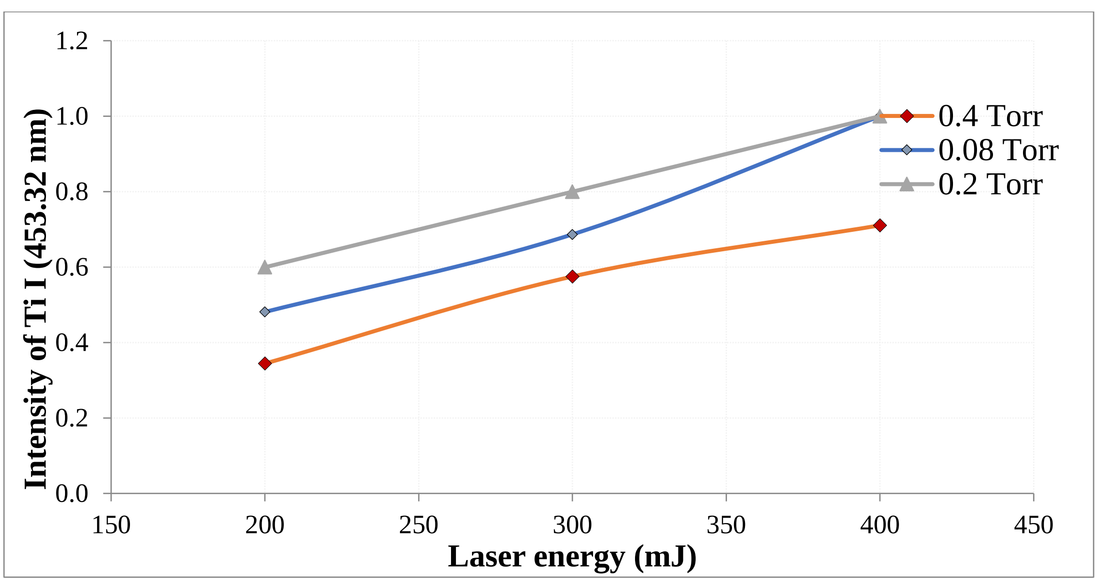

4. Conclusions

In this study, the effect of laser energy and vacuum pressure in Argon of laser-induced spectroscopy from titanium target shows the following aspects. The results showed the possibility of conducting the emission spectroscopy process under a vacuum with good efficiency, but within a specific pressure, which ensures the purity of the measured spectrum from the spectral lines emitted from the components of the atmosphere or the pollutants that may be present in it. It was found that increasing the energy of the used laser increases causes to increase in the emitted line intensity, the plasma density, and the temperature. While increasing the pressure from 0.08 to 0.4 Torr led to a slight decrease in the plasma temperature, while the plasma density increased at 0.2 and decreased at 0.4. Likewise, the emission intensity increased at 0.2 and decreased at 0.4.

References

S. A. Linnik and A. V. Gaydaychuk, Application of optical emission spectroscopy for the determination of optimal CVD diamond growth parameters in abnormal glow discharge plasma, Vacuum **103**, 28–32 (2014).

Z. Machala, M. Janda, K. Hensel, I. Jedlovský, L. Leštinská, V. Foltin, V. Martišovitš, and M. Morvová, Emission spectroscopy of atmospheric pressure plasmas for bio-medical and environmental applications, Journal of Molecular Spectroscopy **243**(2), 194–201 (2007).

M. Ivković, S. Jovićević, and N. Konjević, Low electron density diagnostics: development of optical emission spectroscopic techniques and some applications to microwave induced plasmas, Spectrochimica Acta Part B: Atomic Spectroscopy **59**(5), 591–605 (2004).

A. A. Menazea, Femtosecond laser ablation-assisted synthesis of silver nanoparticles in organic and inorganic liquids medium and their antibacterial efficiency, Radiation Physics and Chemistry **168**, 108616 (2020).

M. Z. Butt, Laser ablation characteristics of metallic materials: Role of Debye-Waller thermal parameter, IOP Conference Series: Materials Science and Engineering **60**(1), 012068 (2014).

S. Marino, S. Palanco, M. Gabás, R. Romero, and J. R. Ramos-Barrado, Laser nano- and micro-structuring of silicon using a laser-induced plasma for beam conditioning, Nanotechnology **26**(5), 055303 (2015).

J. Ciganovic, S. Zivkovic, M. Momcilovic, J. Savovic, M. Kuzmanovic, M. Stoiljkovic, and M. Trtica, Laser-induced features at titanium implant surface in vacuum ambience, Optical and Quantum Electronics **48**(2), 133 (2016).

D. Liu, C. Chen, X. Gao, J. Lin, B. Man, Y. Sun, and F. Li, Effect of ambient pressure on a femtosecond laser induced titanium plasma, European Physical Journal D **70**(11), 1–7 (2016).

"NIST Chemistry WebBook, U.S. department of cmmerce, on line avelable.," .

F. Bredice, P. Pacheco Martinez, C. Sánchez-Aké, and M. Villagrán-Muniz, Temporal evolution of the spectral lines emission and temperatures in laser induced plasmas through characteristic parameters, Spectrochimica Acta Part B: Atomic Spectroscopy **107**, 25–31 (2015).

B. Zmerli, B. Nessib, and M. S. Dimitrijevi, On the Stark broadening of CuI spectral lines, **15**, 152–156 (2010).

V. Unnikrishnan, K. Alti, V. Kartha, C. Santhosh, G. Gupta, and B. Suri, Measurements of plasma temperature and electron density in laser-induced copper plasma by time-resolved spectroscopy of neutral atom and ion emissions, Pramana - Journal of Physics **74**(6), 983–993 (2010).

F. Hall and B. Hill, Introduction to gas discharges, Plasma Sources Science and Technology **9**, 517–527 (2000).